Int. J. Electrochem. Sci., 17 **(2022)** Article Number: 220457, doi: 10.20964/2022.04.40

International Journal of
ELECTROCHEMICAL
SCIENCE
www.electrochemsci.org

Graphite Oxide-Silicone Rubber Composite modified carbon paste electrode as electrochemical sensor for Propranolol determination

Xintao Fu, Zepeng Wang[*]*, Lianxiang Ma*

College of Electromechanical Engineering, Qingdao University of Science and Technology, Qingdao, 266061, China
[*]E-mail: wzp_ww1@126.com,

Received: 29 December 2021 / *Accepted:* 7 February 2022 / *Published:* 4 March 2022

The objectives of this work were to create a graphite oxide (GO) and silicone rubber (SR) composite (GSRC), analyze its mechanical and electrochemical capabilities, and use it to determine propranolol (PRN) electrochemically. The surface morphology and crystal structure of GSRC were studied, and the results showed that a porous GSRC sample was successfully formed. According to a study on mechanical properties, the addition of GO can improve the mechanical qualities of GSRC before and after thermal oxidative aging. The electrochemical properties of the GSRC modified carbon paste electrode (GSRC/CPE) for PRN measurement revealed that it was sensitive, stable, and selective. According to amperometry tests, increasing PRN concentration per step from 1 to 340 M resulted in a linear rise. The detection limit (S/N=3) and sensitivity of 15 nM and 0.2003 A/M, respectively, were obtained. The performance of GSRC/CPE as a PRN sensor was comparable or better than that of some of the recently reported PRN sensors, which was attributed to the synergistic catalytic impact of GO and SR in the composite.

Keywords: Mechanical properties; Silicone rubber; Nanocomposite; Graphite oxide; Amperometry; Propranolol

1. INTRODUCTION

Silicone rubber (SR, polydimethylsiloxane), commonly known as dimethylpolysiloxane or dimethicone, is a long-lasting, high-strength elastomer made up of an inorganic Si-O backbone and polymer chains [1, 2]. Elongation, strong tear strength, outstanding thermal conductivity, and great tolerance to extremely high temperatures, including fire, are all prominent SR features [3, 4]. SR is a flowable liquid that cures to create a flexible silicone elastomer or rubber that is used in a range of applications, including adhesives, sealants, lubricants, varnishes, resins, moulding rubbers for

replication, encapsulants, and potting compounds for electronics and coatings [5, 6]. It can be utilized to bind together major building elements such as concrete, plastics, glass, metal, and granite due to its adhesive characteristics [7]. This improves a structure's strength and durability by protecting it from heat, pollution, moisture, and other damaging elements [8].

Accordingly, the chemical and mechanical properties of SR are important factors in optimizing the its performance efficiency, and many studies have been conducted on the reinforcement of SR by doping, hybrid nanocomposites and micro/nano fillers [9-11]. Reports evidenced that the addition of metal oxide, carbon black, graphene and carbon nanotubes could enhance the thermal, electrical, mechanical and electrochemical properties of SR [12-18]. Therefore, this work was focused on the synthesis of graphite oxide-silicone rubber composite, study of its mechanical and electrochemical properties, and application to the electrochemical determination of propranolol (PRN) [19-21].

PRN (1-[(1-methylethyl)amino]-3-(1-naphthalenyloxy)) is a synthetic beta-adrenergic receptor-blocking drug used to treat excessive blood pressure, tremors, angina, heart rhythm problems, and other heart or circulation issues. It's also used to treat or prevent heart attacks, as well as to lessen the severity and frequency of migraines [22, 23]. However, the most common side effects of PRN are dizziness or fatigue, cold hands or feet, sleeping difficulties, and nightmares. These side effects are usually mild and short-lived. Due to the wide applications and side effects of PRN, it is necessary to develop sensitive and facile procedures for the determination of PRN in clinical applications.

2. EXPERIMENTAL

2.1. Preparation of GSRC

At a volume ratio of 20:80 [24], CPE was made by homogeneously blending graphite powder (98.5%, Zibo Yinxuan Carbon Technology Co., Ltd., China) and paraffin oil (98%, Shandong Green New Materials Co., Ltd., China). A pushing copper wire was put on the other side of the Teflon tube to establish electrical contact after the mixture was stuffed into the end of the cylindrical Teflon tube. The CPE surface was polished with a soft paper after it had cooled. After that, deionized water was used to rinse the polished surface.

For the preparation of GSRC [17, 25], 2g graphite oxide powder (GO, 99%, <20 μm, Sigma-Aldrich) was added to 1g of Silicone Rubber (Fibreglass, New Zealand) insulator phase and 0.5 ml toluene (99%, Sigma-Aldrich), and then it was mechanically homogenized for 15 minutes. Subsequently, the prepared GSRC was slowly dropped onto the CPE surface and dried at room temperature.

2.2. Characterization

The surface morphologies of the produced composites were studied using a scanning electron microscope (SEM, Hitachi X-650, Japan). The crystal structure was studied using an X-ray diffractometer (XRD; D/max-RA, Rigaku, Japan).

The prepared SR and GSRC mixes were cured in a stainless steel mold 3 mm thick with air vents at 175°C under a pressure of 9 MPa for 12 minutes in order to obtain vulcanizates in order to evaluate the mechanical properties of SR and GSRC samples such as tensile strength (TS) and elongation at break (EB). Mechanical properties were investigated at room temperature using a universal testing machine (Hounsfield Series S, UK) with a crosshead speed of 10 mm/min. The as-synthesized vulcanizates were aged in an air-blowing oven at 280 °C for 14 hours for thermal oxidative aging.

Amperometry and differential pulse voltammetry (DPV) experiments were performed using the potentiostat-galvanostat system (Autolab, PGSTAT®model 204 with module FRA32M, Utrecht, The Netherlands) in conventional electrochemical cell which consisted of a Pt plate as counter, Ag/AgCl as reference and bare and modified CPE as working electrode. 0.1 M phosphate buffer solution (PBS, Sigma-Aldrich) with pH 7.4 was used as an electrolyte for electrochemical studies.

3. RESULTS AND DISCUSSION

3.1. Studies of surface morphology and crystal structure

Figure 1 displays SEM images of the GO/CPE and GSRC/CPE morphologies. The SEM picture GO/CPE shows that GO is made up of flakes with a distinctively flaky or platy shape and thin layers with a thickness of less than 100 nm. As seen in this SEM picture, the GSRC/CPE has a rough and porous surface, as well as a good dispersion of flake GO sheets in the SR matrix. There are no agglomerates in the SR, and the particles are perfectly disseminated, exhibiting homogenous nanofiller dispersion in the polymer matrix.

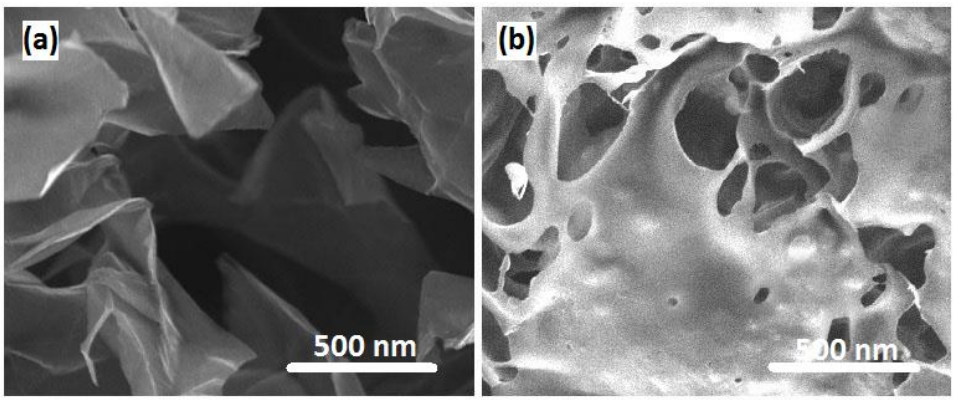

Figure 1. SEM images of morphologies of the (a) GO/CPE and (b) GSRC/CPE.

Figure 2 displays the XRD patterns of GO and GSRC samples. From Figure 2a, the XRD patterns of GO present the sharp diffraction peak at 2θ=25.92° which corresponds to the typical crystal structure of GO with a diffraction line of (002) carbon (JCPDS card No.41-1487) [26, 27]. The XRD patterns of the GSRC sample show an additional weak diffraction peak at 2θ=12.71° which is

attributed to the formation of the fluo-rophlogopite mica amorphous structure of SR (JCPDS card No. 16-0344) [28]. The XRD and SEM observations indicated the successful formation of the porous GSRC sample.

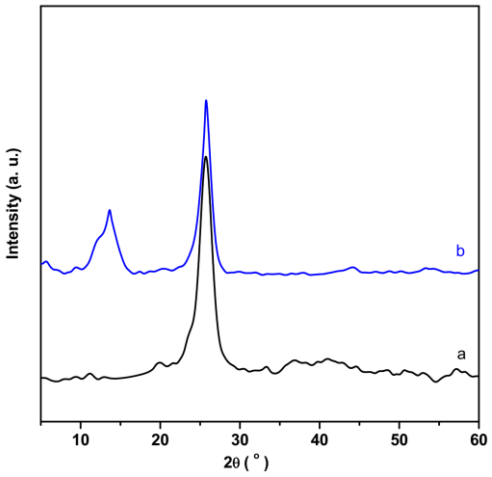

Figure 2. XRD patterns of (a) GO and (b) GSRC samples.

3.2. Study of mechanical property

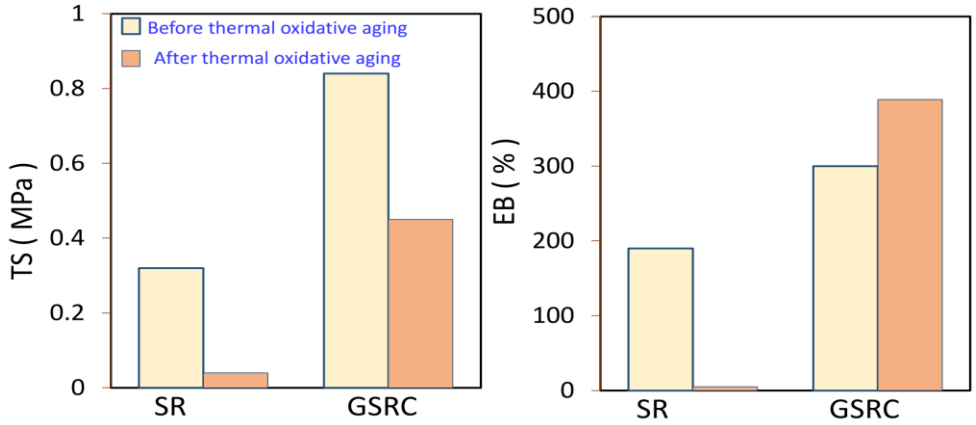

Figure 3. (a) Tensile strength and (b) Elongation at break of SR and GSRC samples before and after thermal oxidative aging

As shown in Figure 3, the mechanical properties of SR and GSRC were investigated before and after thermal oxidative aging. Before thermal oxidative aging, the TS of SR and GSRC samples was 0.32 and 0.84 MPa, respectively (Figure 3a), demonstrating a considerable difference in the TS values of SR and GSRC samples, with the GSRC sample having the greatest value. The SR becomes hard and brittle during thermal oxidative aging. As a result, the TS and EB of the SR sample have been reduced to 0.04 MPa. GSRC's TS has also dropped to 0.45 MPa. Despite the fact that the TS value has decreased, the GSRC sample has a greater value.

The same measurements were conducted on samples for evaluation of the elongation at break. Before thermal oxidative aging, Figure 3b shows that the EB of SR and GSRC samples were 190% and 300%, respectively. After thermal oxidative aging, the EB of SR decreased to 5% and the GSRC increased to 389%. Results demonstrate that the TS and EB values of GSRC are enhanced which is associated with the reinforcement of the well-dispersed flake GO sheets in the SR matrix. Exfoliated GO with a large effective surface area can improve the dispersion and formation of 3D interconnected networks with polymer chains [29-31]. Therefore, GO can promote the mechanical properties of GSRC before and after thermal oxidative aging.

3.3. Study of electrochemical property

Figure 4 shows the findings of DPV investigations of CPE, GO/CPE, and GSRC/CPE in 0.1 M PBS with pH 7.4 containing 1 M PRN at a potential range of -0.5 V to 1.0 V with a scan rate of 15 mV/s in 0.1 M PBS with pH 7.4 containing 1 M PRN at a potential range of -0.5 V to 1.0 V with a scan rate of 15 mV/s. The oxidation peak of CPE, GO/CPE, and GSRC/CPE can be seen in the DPV curves at 0.64 V, 0.61 V, and 0.55 V, respectively. It implies that the hydroxyl group is involved in the PRN oxidation process [32].

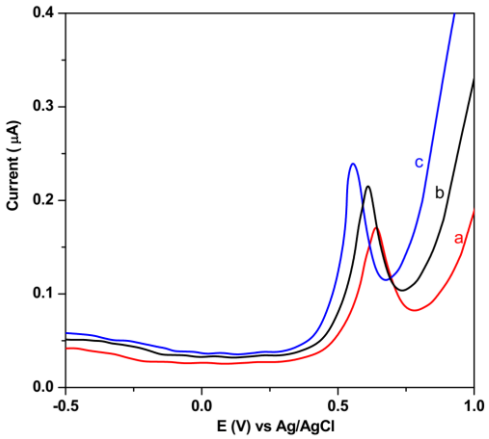

Figure 4. Results DPV studies of (a) CPE, (b) GO/CPE and (c) GSRC/CPE in 0.1 M PBS with pH 7.4 containing 1 µM PRN at potential range from -0.5 V to 1.0 V with a scan rate of 15 mV/s.

As seen, the electrochemical response of GO/CPE is higher than that of CPE which can be related to the sp^2 hybridized carbon of GO which exhibits good adsorption, conductivity and high sensitivity [33, 34]. The presence of C–OH, –COOH, and epoxide functional groups on graphite oxide allows polar molecules and polymers to be easily absorbed [35]. GSRC/CPE has the most sensitive response and the lowest potential. It's most likely due to the roughness and porosity of GSRC, as well as the existence of functional groups in SR polysiloxanes (Si–OH, Si–Cl, Si–OR, etc.) that could interact with the PRN [16, 36]. Because of the flexibility of the backbone –Si–O– in poly (dimethylsiloxane), the SR serves as a more stable nonporous membrane with higher permeability than

almost all other materials [37], and covalent binding of ion-recognition sites to the conducting polymer backbone provides integration of ion-recognition sites and an ion-to-electron transducer [38]**.** The backbones of silicone SR also contain Si–O–Si units with polarity because of the differences in electronegativity between silicon and oxygen [35]. Therefore, the conductivity and polarity of graphite and SR can enhance the electrochemical signal and shift the oxidation potential towards the negative direction [39-41].

At potentials ranging from -0.5V to 1.0V and a scan rate of 15mV/s, the stability of the electrochemical response of GSRC/CPE was investigated. Figure 5 shows the GSRC/first CPE's and 60th DPV responses, revealing that the electrochemical reaction has dropped by less than 3.7% after 60 scans. The remarkable stability of the GSRC/CPE electrochemical reaction is attributed to the strong stability of Si–O–Si in the SR backbone [42].

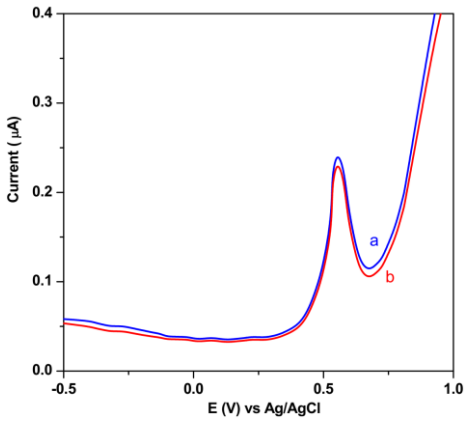

Figure 5. (a) The initial and (b) 60th Electrochemical DPV response of GSRC/CPE in 0.1 M PBS with pH 7.4 containing 1 µM PRN at potential range from -0.5 V to 1.0 V with a scan rate of 15 mV/s.

Figure 6a displays the amperometric response of GSRC/CPE to consecutive injections of 20 µM PRN at a potential of 0.55 V under stirring at a speed of 1000 rpm in 0.1 M PBS with pH 7.4. It is found that the GSRC/CPE illustrates a relatively rapid response to any addition of PRN solution, and the amperometric response curve of GSRC/CPE depicts a linear increase for increasing PRN concentration of 20 µM per step with successive addition of PRN from 1 to 340 µM in 0.1 M PBS. The calibration plot in Figure 6b yields a detection limit of 15 nM (S/N=3) and a sensitivity of 0.2003 µA/µM. Table 1 compares the results obtained here with some of the recently reported PRN sensors. It shows the comparable or better performance of GSRC/CPE as a PRN sensor, which is ascribed to the synergistic catalytic effect of GO and SR in composite.

Various possible interfering substances which are most commonly found compounds in a wide range of real pharmaceutical samples were investigated for their effects on the electrochemical determination of PRN using amperometric measurements of GSRC/CPE to consecutive injections of

10 µM PRN and 50 µM of interfering substances at a potential of 0.55 V under stirring at a speed of 1000 rpm in 0.1 M PBS with pH 7.4. Results are summarized in Table 2 and shows that there is a significant response for PRN, and negligible interference is observed for all pharmaceutical compounds. Therefore, the present sensor could be used for the rapid and selective detection of PRN.

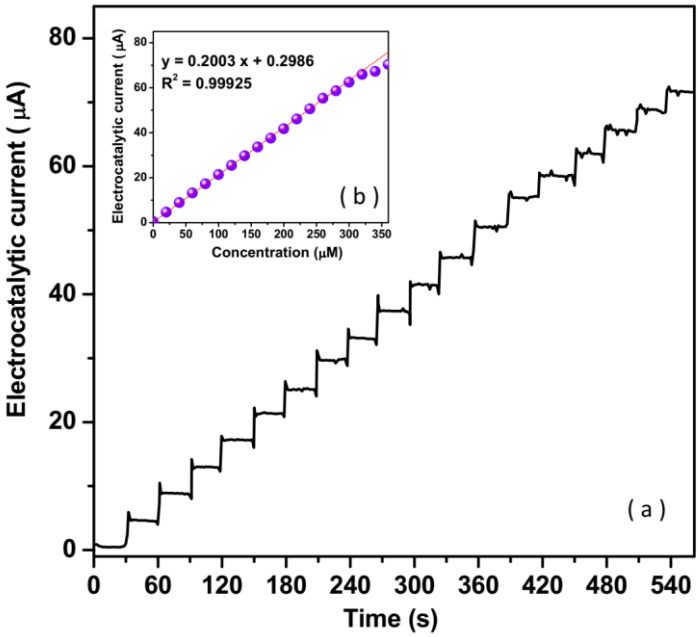

Figure 6. (a) Amperometric response of GSRC/CPE to consecutive injections of 20 µM PRN at potential of 0.55 V under stirring at speed of 1000 rpm in 0.1 M PBS with pH 7.4, and (b) the obtained calibration plot.

Table 1. Comparison the results obtained here with some of the recently reported PRN sensors.

Electrodes	Technique	Detection limit (nM)	Linear range (µM)	Ref.
GSRC/CPE	AMP	15	1–340	This study
Ag NPs/ionic liquid/functionalized graphene/GCE	DPV	17	0.1–2.9	[43]
CuO NPs/CPE	DPV	2900	10–104	[44]
Graphene/(poly-1,5-diaminonaphthalene)/EPPG	SWV	20	0.1–750	[45]
Magnetic core-shell manganese ferrite NPs	DPV	80	0.4 – 200	[46]
molecularly imprinted polymer NPs/CPE	EIS	80	0.1–10	[47]
Pt NPs/MWCNTs	DPV	84.5	0.67–38	[48]
HgS/graphene/GCE	DPV	50	0.5–50	[49]
MWCNTs/GCE	DPV	1370	4.22-135	[50]
8-hydroxy-8-propoxy-calix [8] arene /MWCNT	DPV	135	0.338–54.1	[51]
3D Au NPs/Au	DPV	67500	0.1–20	[52]

GCE: Glassy carbon electrode; EPPG: Edge plane pyrolytic graphite; SWV: Squarewave voltammetry; EIS: Electrochemical impedance spectroscopy

Table 2. Results of study the interfering effect of most commonly pharmaceutical compounds on the amperometric determination of PRN using GSRC/CPE at potential of 0.55 V under stirring at speed of 1000 rpm in 0.1 M PBS with pH 7.4.

Substance	**Added (µM)**	**Current (µA) at 0.55 V**	**RSD (%)**
PRN	10	2.029	±0.077
Ascorbic Acid	50	0.128	±0.018
Leucine	50	0.220	±0.011
Uric acid	50	0.211	±0.018
Sorbitol	50	0.222	±0.012
Benzoic acid	50	0.704	±0.029
Citric acid	50	0.205	±0.010
Starch	50	0.198	±0.011
Glucose	50	0.110	±0.015
Maltodextrin	50	0.251	±0.008
Fructofuranose	50	0.144	±0.009
Dextrose	50	0.304	±0.012
Glycine	50	0.451	±0.038
Dopamine	50	0.305	±0.012
Manitol	50	0.364	±0.037
Lactose	50	0.072	±0.007
Folic acid	50	0.110	±0.010
Carboxymethylcellulose	50	0.105	±0.012
Urea	50	0.102	±0.013
Ca^{2+}	50	0.108	±0.015
Cu^{2+}	50	0.208	±0.009
$SiO^{4-}{}_4$	50	0.229	±0.010
Na^{+}	50	0.094	±0.008
SO_4^{2-}	50	0.207	±0.011
Mg^{2+}	50	0.155	±0.013

4. CONCLUSION

The synthesis of GSRC, the assessment of mechanical and electrochemical properties, and the application of GSRC modified CPE to the electrochemical measurement of PRN have all been demonstrated in this study. The results of SEM and XRD showed that the porous GSRC sample was successfully formed. According to the results of mechanical characterization, the addition of GO can improve the mechanical properties of GSRC before and after thermal oxidative aging. The electrochemical properties of GSRC/CPE showed that it can be used as a sensitive, stable, and selective electrochemical PRN sensor, and a comparison of the results obtained sensing properties with some of the recently reported PRN sensors revealed that GSRC/CPE has comparable or better

performance as a PRN sensor, which was attributed to the synergistic catalytic effect of GO and SR in the composite.

ACKNOWLEDGMENTS
This research was funded by the National Natural Science Foundation of China (No. 51576102) and Natural Science Foundation of Shandong Province (No. ZR2019MEM050).

References

1. W. Du, Z. Zhang, W. Fan, W. Gao, H. Su and Z. Li, *Materials & Design*, 158 (2018) 28.
2. H. Maleh, M. Alizadeh, F. Karimi, M. Baghayeri, L. Fu, J. Rouhi, C. Karaman, O. Karaman and R. Boukherroub, *Chemosphere*, (2021) 132928.
3. Q. Hu, X. Bai, C. Zhang, X. Zeng, Z. Huang, J. Li, J. Li and Y. Zhang, *Composites Part A: Applied Science and Manufacturing*, 152 (2022) 106681.
4. X. Zhang, Y. Tang, F. Zhang and C.S. Lee, *Advanced energy materials*, 6 (2016) 1502588.
5. Q. Wei, D. Yang, L. Yu, Y. Ni and L. Zhang, *Composites Science and Technology*, 199 (2020) 108344.
6. M. Khosravi, *Journal of Eating Disorders*, 8 (2020) 1.
7. C. Zhao, M. Xi, J. Huo, C. He and L. Fu, *Materials Today Physics*, 22 (2022) 100609.
8. J. Zhang, Y. Zhao, Y. Liu, C. Zhu, B. Wang, L. Zhang, G. Li, H. Wu, C. Liu and Y. Li, *Journal of Alloys and Compounds*, 902 (2022) 163723.
9. K.E. Polmanteer, *Rubber chemistry and technology*, 61 (1988) 470.
10. G. Momen and M. Farzaneh, *Reviews on Advanced Materials Science* 27 (2011) 1.
11. A. Bahrami, A. Nateghian, S. Salehi, G. Bahoush, S. Talebi, S. Ghasemi, S. Razi and N. Rezaei, *Acta Medica Iranica*, 58 (2020) 38.
12. Y. Hosono, Y. Yamashita and K. Itsumi, *IEEE transactions on ultrasonics, ferroelectrics, and frequency control*, 54 (2007) 1589.
13. Y. Song, J. Yu, L. Yu, F.E. Alam, W. Dai, C. Li and N. Jiang, *Materials & Design*, 88 (2015) 950.
14. H. Hu, L. Zhao, J. Liu, Y. Liu, J. Cheng, J. Luo, Y. Liang, Y. Tao, X. Wang and J. Zhao, *Polymer*, 53 (2012) 3378.
15. L. Wang, F. Ma, Q. Shi, H. Liu and X. Wang, *Sensors and Actuators A: Physical*, 165 (2011) 207.
16. R.A. Sousa, S.X. Dos-Santos, E.T. Cavalheiro and C.M. Brett, *Electroanalysis*, 25 (2013) 706.
17. A.L. Silva, M.M. Corrêa, G.C. de Oliveira, P.P. Florez-Rodriguez, C.A. Rodrigues Costa, F.S. Semaan and E.A. Ponzio, *Journal of Alloys and Compounds*, 691 (2017) 220.
18. Y. Orooji, B. Tanhaei, A. Ayati, S.H. Tabrizi, M. Alizadeh, F.F. Bamoharram, F. Karimi, S. Salmanpour, J. Rouhi and S. Afshar, *Chemosphere*, 281 (2021) 130795.
19. H. Karimi-Maleh, Y. Orooji, F. Karimi, M. Alizadeh, M. Baghayeri, J. Rouhi, S. Tajik, H. Beitollahi, S. Agarwal and V.K. Gupta, *Biosensors and Bioelectronics*, 184 (2021) 113252.
20. M. Khosravi, *Open Access Macedonian Journal of Medical Sciences*, 8 (2020) 553.
21. L. Jiang, Y. Wang, X. Wang, F. Ning, S. Wen, Y. Zhou, S. Chen, A. Betts, S. Jerrams and F.-L. Zhou, *Composites Part A: Applied Science and Manufacturing*, 147 (2021) 106461.
22. S. Salehi, M. Kamali and M. Radgoodarzi, *Progress in Pediatric Cardiology*, 62 (2021) 101378.
23. H. Liu, X. Li, Z. Ma, M. Sun, M. Li, Z. Zhang, L. Zhang, Z. Tang, Y. Yao and B. Huang, *Nano Letters*, 21 (2021) 10284.

24. R.R. Naik, B.K. Swamy, U. Chandra, E. Niranjana, B. Sherigara and H. Jayadevappa, *International Journal of Electrochemical Science*, 4 (2009) 855.
25. S.X.d. Santos, É.T. Cavalheiro and C.M. Brett, *Electroanalysis*, 22 (2010) 2776.
26. R. Siburian, H. Sihotang, S.L. Raja, M. Supeno and C. Simanjuntak, *Oriental Journal of Chemistry*, 34 (2018) 182.
27. X. Du, W. Tian, J. Pan, B. Hui, J. Sun, K. Zhang and Y. Xia, *Nano Energy*, 92 (2022) 106694.
28. F. Lou, L. Cheng, Q. Li, T. Wei, X. Guan and W. Guo, *RSC advances*, 7 (2017) 38805.
29. S. Zhao, L. Bai and J. Zheng, *Materials Research Express*, 5 (2018) 015301.
30. M. Khosravi, *Current Psychology*, 40 (2021) 5735.
31. M.A. Delavar and P. Karimian, *Pakistan Journal of Medical & Health Sciences*, 14 (2020) 1686.
32. L. Chen, K. Li, H. Zhu, L. Meng, J. Chen, M. Li and Z. Zhu, *Talanta*, 105 (2013) 250.
33. H.T. Purushothama, Y.A. Nayaka, M.M. Vinay, P. Manjunatha, R.O. Yathisha and K.V. Basavarajappa, *Journal of Science: Advanced Materials and Devices*, 3 (2018) 161.
34. S. Khosravi and S.M.M. Dezfouli, *Journal of Critical Reviews*, 7 (2020) 275.
35. X. Wang and W. Dou, *Thermochimica acta*, 529 (2012) 25.
36. Y. Jing, H. Niu and Y. Li, *Polymer*, 172 (2019) 117.
37. M. Xiao, J. Zhou, Y. Tan, A. Zhang, Y. Xia and L. Ji, *Desalination*, 195 (2006) 281.
38. J. Bobacka, *Electroanalysis: An International Journal Devoted to Fundamental and Practical Aspects of Electroanalysis*, 18 (2006) 7.
39. Z. He, L. Shi, J. Shen, Z. He and S. Liu, *International Journal of Energy Research*, 39 (2015) 709.
40. D. Bao, B. Millare, W. Xia, B.G. Steyer, A.A. Gerasimenko, A. Ferreira, A. Contreras and V.I. Vullev, *The Journal of Physical Chemistry A*, 113 (2009) 1259.
41. S.M.M. Dezfouli and S. Khosravi, *Indian Journal of Forensic Medicine and Toxicology*, 15 (2021) 2674.
42. F. Wu, B. Chen, Y. Yan, Y. Chen and M. Pan, *Polymers*, 10 (2018) 522.
43. A.M. Santos, A. Wong and O. Fatibello-Filho, *Journal of Electroanalytical Chemistry*, 824 (2018) 1.
44. N. Shadjou, M. Hasanzadeh, L. Saghatforoush, R. Mehdizadeh and A. Jouyban, *Electrochimica acta*, 58 (2011) 336.
45. P. Gupta, S.K. Yadav, B. Agrawal and R.N. Goyal, *Sensors and Actuators B: Chemical*, 204 (2014) 791.
46. S.Z. Mohammadi, S. Tajik and H. Beitollahi, *Indian Journal of Chemical Technology*, 27 (2020) 73.
47. T. Alizadeh and L. Allahyari, *Electrochimica Acta*, 111 (2013) 663.
48. Z. Kun, H. Yi, Z. Chengyun, Y. Yue, Z. Shuliang and Z. Yuyang, *Electrochimica Acta*, 80 (2012) 405.
49. M. Ahmadi-Kashani and H. Dehghani, *Journal of Pharmaceutical and Biomedical Analysis*, 194 (2021) 113653.
50. I. Baranowska and M. Koper, *Journal of the Brazilian Chemical Society*, 22 (2011) 1601.
51. Z. Kun, Y. Shuai, T. Dongmei and Z. Yuyang, *Journal of Electroanalytical Chemistry*, 709 (2013) 99.
52. T. Łuczak, *Ionics*, 25 (2019) 5515.